20030129060

DTIC FILE COPY

AD-A195 824

DOCUMENTATION PAGE

Form Approved OMB No. 0704-0188

1a. REPORT SECURITY CLASSIFICATION (u)	1b. RESTRICTIVE MARKINGS
2a. SECURITY CLASSIFICATION AUTHORITY NA	3. DISTRIBUTION/AVAILABILITY OF REPORT
2b. DECLASSIFICATION/DOWNGRADING SCHEDULE NA	
4. PERFORMING ORGANIZATION REPORT NUMBER(S)	5. MONITORING ORGANIZATION REPORT NUMBER(S)
6a. NAME OF PERFORMING ORGANIZATION: Osborn Labs of Marine Sciences	6b. OFFICE SYMBOL (If applicable): NA
6c. ADDRESS (City, State, and ZIP Code): West 8th Street & Surf Avenue, Brooklyn, N.Y. 11224	7a. NAME OF MONITORING ORGANIZA
7b. ADDRESS (City, State, and ZIP Cod	
8a. NAME OF FUNDING/SPONSORING ORGANIZATION: Office of Naval Research	8b. OFFICE SYMBOL (If applicable)
8c. ADDRESS (City, State, and ZIP Code): 800 N. Quincy Street, Arlington, Virginia 22217-5000	9. PROCUREMENT INSTRUMENT IDENT. N00014-82-C-0435
	10. SOURCE OF FUNDING NUMBERS: PROGRAM ELEMENT NO. / PROJECT NO. / TASK NO. / WORK UNIT ACCESSION NO.

DTIC ELECTE JUN 24 1988 H

11. TITLE (Include Security Classification)

(u) Structure and Mode of Action of the Shark Repellent Pardaxin

12. PERSONAL AUTHOR(S)
Dr. Naftali Primor

13a. TYPE OF REPORT	13b. TIME COVERED	14. DATE OF REPORT (Year, Month, Day)	15. PAGE COUNT
FINAL	FROM 1985 TO 1988	June 5, 1988	

16. SUPPLEMENTARY NOTATION

17. COSATI CODES			18. SUBJECT TERMS (Continue on reverse if necessary and identify by block number)
FIELD	GROUP	SUB-GROUP	Structure and Mode of Action of Shark Repellent Pardaxin
08			

19. ABSTRACT (Continue on reverse if necessary and identify by block number)

Pardaxin, a marine neurotoxic polypeptide, isolated from the secretions of the flatfish Pardachirus marmoratus or synthesized by the solid phase method is a single chain, acidi amphipathic polypeptide with the sequence: NH_2-G-F-F-A-L-I-P-K-I-I-S-S-P-L-F-K-T-L-L-S-A-V-G-S-A-L-S-S-S-G-G-Q-E. Pardaxin is secreted via secretory ducts to the water. Pardaxin repels sharks and the gills and the pharynx are the target organs. On a molecular level, pardaxin forms voltage dependent, cation and anion permeable pores. Model of the pardaxin pore support an antiparallel oligomer of the helical segments with a narrow, negatively charged entrance due to the carboxy terminal segments. Pardaxin seem to be a suitable tool to investigate the molecular structures underlying channel selectivity and voltage dependence, and the relationship between channel activity, cytotoxicity and repellency to marine organisms. (KT).

20. DISTRIBUTION/AVAILABILITY OF ABSTRACT	21. ABSTRACT SECURITY CLASSIFICATION
☒ UNCLASSIFIED/UNLIMITED ☐ SAME AS RPT ☐ DTIC USERS	(u)
22a. NAME OF RESPONSIBLE INDIVIDUAL: Dr. M. Marron	22b. TELEPHONE (Include Area Code): 202-696-4038 / 22c. OFFICE SYMBOL: ONR

DD Form 1473, JUN 86 — Previous editions are obsolete. — S/N 0102-LF-014-6603 — SECURITY CLASSIFICATION OF THIS PAGE

88 6 15 000

DISTRIBUTION STATEMENT A

Approved for public release; Distribution Unlimited

Final Report on Contract N00014-82-C-0435

Principal Investigator: Dr. Naftali Primor

Assisted By: Dr. Philip Lazarovici; Dr. Jay Fox; Dr. Joe Gennaro; Dr. H.R. Guy; Dr. Y.L. Shih; Dr. C. Edwards

Contractor: New York Zoological Society

Contract Title: Pardaxin's Action in Sharks

Start Date: June 1, 1985

1. Moses Sole - Source of Shark Repellents.

Certain ichthyocrinotoxic fish secrete toxic compounds that repel their predators. The Red Sea Moses Sole, Pardachirus marmoratus (Fig. 1a,b) exudes a fluid from specialized glands (Fig. 1) into the surrounding ocean water. This secretion repels sharks, and it has been suggested that it functions as a naturally occurring weapon of defense against shark predation. The principle factors in the secretion is a polypeptide named pardaxin.

2. The Morphology of the Moses Sole Toxins Secretory Apparatus.

Moses sole secretion is secreted by a double row of small cylindrical simple acinar glands (Fig. 1b), one located epaxially and the other hypaxially between each of the fin rays from head to tail (Fig. 1b). The ventral member of the pair of glands releases its secretion from a pore located on the ventral side of the fish, more

peripheral (lateral) to that of its dorsal partner (Fig. 1c). Each cylinder contains a central channel (Fig. 1c,f) which is part of the secretory duct and is lined with interdigitating epithelial cells of the type found in glands in which water is withdrawn from the secretion before it is released (Fig. 1c-e). The outside periphery of the cylinder houses a prominent capillary network and the secretory acini lined by thin secretory cells which surround the acinus, a compartment filled with the secretion. Together these pairs of secretory unites comprise an appreciable portion of the body mass of this small flatfish.

A light microscope image through a longitudinally sectioned pair of toxin secreting glands, shows acini in each gland, although the epaxial gland contains more secreted material than the hypaxial one (Fig. 1c). The secretory duct lies within the plane of the fin ray (the midaxial plane), the center of each gland the articulation of which can be seen in the left of the image, separates both glands.

An electronmicrograph of one acinus shows a large mass of stored secretory material and, adjacent to this is the thin cytoplasm of the almost flat secretory cell (Fig. 1e). The secretion is released into the acinar pool from the secretory cell as globules (Fig. 1d,e) some of which can be seen elevating the plasma membrane of the cells. No secretory granules were present within the cytoplasm of the epithelial cell (Fig. 1e), which contained mitochondria, smooth endoplasmic reticulum and an extensive and dense network of intermediate filaments, probably keratin. The acinus was surrounded by a system of

satellite cells (cells with pleomorphic nuclei) applied closely to them with no intervening amorphous basement material. Instead both amorphous and reticular components of the basement material were peripheral to the satellite cell. An electronmicrograph of the epithelium lining the secretory duct shows the irregular rounded apical elevations which protrude into the duct space and the complexity of the interdigitations along their lateral boundaries (Fig. 1f). These structures possess a peculiar electron density subadjacent to the plasma membrane and under that a cytoplasm rich in electron dense particles with endoplasmic membranes. The other most conspicuous structural feature of these cells was the complex nature of their interdigitation in the region of their lateral boundaries. Many mitochondria with prominent cristae were present in the basal regions of some duct cells. This entire constellation of structures suggests energy production to support an active ion transport process.

3. Pardaxin Sequence, Secondary Structure Predictions and Modeling in Water Solutions.

Pardaxin is a single chain, acidic, amphipathic, hydrophobic polypeptide, composed of 33 amino acids and with a mass of 3500 daltons:

NH_2 - Gly - Phe - Ala - Leu - Ile - Pro - Lys - Ile - Ile - Ser - Ser - Pro - Ile - Phe - Lys - Thr - Leu - Leu - Ser - Ala - Val - Gly - Ser - Ala - Leu - Ser - Ser - Ser - Gly - Gly - Glu - COOH.

The hydrophobic mement plot of pardaxin residue values, based on the consensus hydrophobicity scale, indicates that most of the points fall on or near the surface region. Its highly hydrophilic carboxy terminal lie in the globular region. This property is typical for surface-seeking, amphiphilic proteins which have large helical hydrophobic moments, such as melittin, Staphylococcus aureus delta toxin and other cytolysins.

Possible secondary structures of pardaxin were predicted by the Delphi program using decision constants (DHA = -75, DHE = 50) that favor a helices over extended segments and by the Amphi program (Guy, unpublished data) that identified possible amphipathic a helices and b strands. Delphic predicted that pardaxin segments 1-8 and 16-25 were a helices and the remainder may be coil or turns. Amphic predicted that segments 1-12 and 13-28 could form amphipathic a helices. Pardaxin is predominantly found in different oligomeric forms in aqueous solutions and like melittin, binds deoxycholate and most probably dissociates from a tetramer to a monomer upon interaction with detergent micelles. This possibility is strongly supported by the results of crosslinking experiments, the spontaneous aggregation seen with gel electrophoresis and the higher susceptibility of pardaxin oligomers to proteolysis in the presence of deoxycholate. The mechanism may be the same as that responsible for the aggregation of typical integral membrane proteins in aqueous buffers in the absence of lipid or detergents.

Approximate three dimensional models of pardaxin aggregates, were developed using computer graphics. These models were then used as starting points for energy refinement calculations to obtain more precise models. In the models presented here (Fig. 2 & 6) pardaxin had two a helical segments, the N-helix and the C-helix comprised of residues 2-10 and 15-29. These segments were assigned helical structures for the following reasons: 1) Proline is frequently found in the first position of a helices and Pro-13 is immediately followed by residues that are frequently observed in a helices, 2) initial models indicated that adjacent a helices pack well next to each other when the C-helix extends to residue 29, and 3) the segment 11-13 (Ser-Ser-Pro) is strongly predicted not to be in a helical conformation and the residues that precede a proline are not usually an a helical conformation. The initial C-helix was created by a program that generated a helices with the backbone structure and side chain conformations most commonly observed for a helices in crystal structures. This program was not appropriate for an a helix that contains an interior proline. The initial backbone structure, the N-helix, was modeled from the a helical segment 120-128 in lactate dehydrogenase (13) with the sequence PHE-lys-phe-Ile-ILE-PRO-asn-ILE-Val in which most residues were identical or similar to those of the pardaxin segment 2-10 as indicated by capitals and underlining. The remaining C-terminus residues were assigned phi and psi backbone torsion angles commonly observed in random coil segments and that extended the Glu-33 carboxyl groups into a region postulated to be occupied by water and near Lys-8 and Lys-16 of adjacent helices. Initially, the conformations of

Ser-11 and Ser-12 were adjusted manually using computer graphics to that N-helices could have apparently favorable interactions with the membrane lipid and with other protein segments. Connolly surfaces were added to the structures and monomers were manually docked to form channel structures using the Mogli program on an Evans and Sutherland computer graphics monitor. C-helices were packed so that Connolly surfaces formed a tight barrier between the inside and outside of the channel. Most hydrophilic groups not involved in internal hydrogen bonds were positioned to be exposed to water and most hydrophobic groups were positioned to be in contact with the hydrocarbon portion of the lipid membrane. Energies for individual dimers created this way were refined with the CHARMM program using adopted basic Newton-Raphson method. A conversion criterion of .01 angstroms was used for the rms gradient during a cycle of minimization. These energy refined dimers were then used to reconstruct aggregates and a final energy refinement was performed on the complete aggregate. Each monomer was in an identical environment and had the same conformation.

In solution pardaxin appears to exist primarily as a tetramer. A tetramer (Fig. 2) and a "raft" model were developed using dimers that have the same packing for the C-helices as the channel model. The major differences among the monomer conformations of these models involve the C-terminus and residues Ser-11 and Ser-12 that control the relative positions of the N- and C- helices to each other. In the tetramer the dimers were packed next to each other so that the row of large hydrophobic side chains on the C-helices of each dimer packed next to those of the adjacent dimer (Fig. 2). This produced a

structure similar to that of melittin tetramers. The tetramer structure had 2-fold symmetry about each orthoganal axis (Fig. 2). Helical interactions between C-helix dimer had "4-4 ridges-into-grooves" type packing. The N-helices were positioned so they fit into a hydrophobic groove formed by the C-helices. The N-termini of two N-Helices approached each other on each side of the tetramer. All hydrophilic side chains were exposed on the surface and most hydrophobic side chains were buried. This model was in accordance with the unique property of pardaxin to reduce water surface tension at concentrations more than 10^{-6} M, the critical micellar concentration of this peptide in aqueous solutions.

4. Mechanism of Pardaxin Produced Repellency.

4.1 Location of the Pardaxin Target in Fish.

In free-swimming sharks, mixing bait with the gland secretion stops the shark from completing its bite and causes it to leave with an abnormally open jaw. In sharks, the main organ for chemical sensation is located within the lateral-line organ of the head. To determine whether the response to pardaxin was mediated through the lateral line system or via the pharyngeal cavity and the gills, an apparatus was constructed which prevented a mixing of the outflow from shark gills with water bathing its surface skin. Pardaxin administered to the medium bathing the shark's head skin surface did not elicit observable behavioral repellent responses. When added to the medium bathing the shark's pharynx and gills, PX immediately

caused the shark to struggle violently. It was rather unexpected to find that the shark's main sensory system, located at the head surface, did not respond to PX's. Furthermore, pardaxin elicited its repellent effect only when administrated in sea water to the skin of the shark and showed no effect when injected into the circulation. Previous studies have shown that Na^+-K^+ ATPase of the gills of teleost fish are affected by pardaxin and hystopathological effects have been described.

4.2 Pardaxin Impairment of Ion-Transport in the Killifish Opercular Epithelium.

Since pardaxin affects gills in both teleosts and elasmobranchs and its toxicity is elevated in fish preadapted to a medium of high salinity its mode of action was examined by studying its effect upon ionic transport by the opercular epithelium of the killifish Fundulus heteroclitus. Administration of pardaxin to the mucosal (seawater) side of the isolated shortcircuited opercular epithelium caused a transient stimulation of the active transport of ions (I_{sc}), followed by an inhibition (Fig. 3). The stimulation was abolished by ouabain and/or removal of Na^+ from the Ringer but not in Cl^- or HCO_3^- Ringer. Pardaxin did not affect the I_{sc} when applied to the serosal (blood) side. On the mucosal side, pardaxin produced a net transient Na^+ current from the mucosal side to the serosal side of 2.2 μequiv $cm^{-2}h^{-1}$. It was concluded that the increased Na^+ influx underlay the Isc stimulation, and was suggested to be the mechanism responsible for the toxicity of pardaxin.

4.3 Pardaxin Evoked Increase in Intracellular Ca^{2+} in Chromaffin Cells.

The effect of pardaxin on intracellular free Ca^{2+} concentrations, was examined using chromaffin cells. The basal level of $[Ca^{2+}]$ in these cells was found to be 50-90 nM. Stimulation of the cells with potassium triggered rapidly a transient $[Ca^{2+}]$ in peak which gradually declined to the resting $[Ca^{2+}]$ in value (Fig.4). As expected, ionomycin, a calcium ionophore caused a sustained rise in the free intracellular concentration to approximately 450 nM (Fig.4). In this system, pardaxin induced a fluorescence response of Fura 2-loaded cells only in the presence of extracellular Ca^{2+} (Fig. 4). These results indicated that pardaxin mediated a Ca^{2+} influx but did not release Ca^{2+} from intracellular stores. This influx is most probably mediated directly by pardaxin pores and probably also indirectly by chromaffin cells Ca^{2+} channels activated by the depolarization process of pardaxin pores. These observations further substantiate our hypothesis that transmembrane fluxes of Na^{+}, K^{+} and also of Ca^{2+} are involved in the pathological action of pardaxin.

4.4 Presynaptic Effects Of Pardaxin.

The effects of pardaxin on neuromuscular transmission was examined using the frog sartorius nerve muscle preparation. Pardaxin produced pre- but not postsynaptic neurotoxic effects. It increased the frequency of the spontaneous release of transmitter quanta in a dose-dependent and temperature-influenced way up to more than 100

times control values. At the same time the quantal content of the evoked end-plate potentials was greatly elevated. The glycosteroids isolated from the gland secretion were relatively ineffective on neurotransmitter release; however, at high doses they had postsynaptic effects, as shown by a diminution of the amplitude of the evoked end-plate potentials. They did not reinforce the effect of the pardaxin. At higher doses pardaxin induced depolarization of postsynaptic membranes, and muscle contractions he produced could not be blocked by (+)-tubocurarine or by tetrodotoxin. No effects on nerve conduction were observed.

This profound presynaptic activity of pardaxin led us to suggest that pardaxin may act on the seawater-facing cells of the gills and/or the pharynx by two mechanisms: 1) Repellency (10^{-6} - 10^{-8} M) as a result of depolarization and activation of sensory-motor neuronal pathways involved in the escape behavior, and 2) toxicity (10^{-6} - 10^{-4} M) as a result of the collapse of the osmoregulatory homeostasis of the fish.

5. Ionophore Activity Of Pardaxin.

5.1 Pore Forming Activity In Liposomes.

When a pore forming factor inserts into the hyperpolarized membrane of lipid vesicles, ion gradients are rapidly dissipated, leading to complete depolarization. A potentiometric cyanine dye was used to elucidate some of the characteristics of pardaxin pore in

phosphatidylcholine liposomes. Pardaxin made a more complex channel (10^{-10} - 10^{-9} M), ›ared to gramicidin, a well known ionophore. This pardaxin channel does not discriminate significantly between cations and anions and it is equally effective if sucrose or choline sulfate replaces the Na_2 So_4 in the external buffer. From the fraction of depolarized vesicles it was estimated that 4-12 pardaxin monomers are required to discharge the ion gradients across the liposomal membrane.

5.2 Aggregation Of Phosphatidylserine Vesicles By Pardaxin.

Besides forming pores in lipid membranes, pardaxin induces aggregation of phosphatidylserine vesicles, a phenomena which we have visualized with negative contrast electron microscopy. Pardaxin induced aggregation is very rapid and continues for an extended period of time (> 30 min). Furthermore, pardaxin induced aggregation is strongly modulated by the transmembrane and/or surface potential. In spite of the extensive aggregation, no exchange of lipids between vesicles or fusion was observed. We have proposed that vesicle aggregation is probably related to the state of binding, insertion, aggregation and/or conformation of pardaxin in the phosphatidylserine vesicle lipid bilayer. This conclusion is supported by the observation that phosphatidycholine vesicles are not induced to aggregate and that the pardaxin induced phosphatidylserine vesicle aggregation is affected by charge polarization of the vesicle. This suggestion seems to be consistent also with the voltage dependence of

fast "pore" activity of pardaxin, the channels which are open only at positive membrane potentials.

5.3 Single Channel Recordings And Selectivity Of Pardaxin Channels On Planar Bilayers Of Ethanolamine At The Tip OF PATCH PIPETS.

To learn about the ion selectivities of the pardaxin channels, its behavior in lipid bilayers was examined. Bilayers of phosphatidylethanolamine were formed at the tips of micropipettes (Fig.5a) by the double-dip method. After the bilayer was found to be stable, pardaxin was added to the solution on one side, whose potential was set at +20 mV. The currents across the bilayer in the voltage clamp mode were monitored. At low concentrations of pardaxin (10^{-9} - 10^{-8} M) single channel events (Fig. 5b) usually appeared within 10-20 minutes. At higher concentrations the latencies were shorter. A potential gradient was required for the pardaxin molecules to insert and/or express channel activity into the membrane; little or no activity was found in the absence of a potential gradient.

To determine the ionic selectivity of the pardaxin channels, various ion substitutions were performed and the bionic reversal potential, i.e., the potential at which the current across a bilayer with many open pardaxin channels changed sign, was determined. The relative permeabilities of the ions could then be determined from the general equation:

$$E_{rev} = \frac{RT\ Pc_1[C_1]+PA_1[A_1]}{nF\ Pc_2[C_2]+PA_2[A_2]}$$

Where C_1, C_2, A_1 and A_2 are the concentrations of cations and anions on sides one and two. In practice, it was found that Tris was an impermeant cation and HEPES an impermeant anion, and so salts of these compounds were used to simplify the experimental conditions. For cations the selectivity sequence was $Tl^+ > Cs^+ > Rb^+ > K^+ > NH_4^+ > Li^+ Na^+$ which, except for Li^+, is the same as that of the relative hydrated sizes. For anions the sequence was $I^- > NO_3^- > Br^- > Cl^- > ClO_4^- > SCN^- > HCOO^-$, which is quite different from that of the relative hydrated sizes. Therefore, the mechanisms governing the permeabilities of cations and anions appear to be different.

5.4 Modeling Pardaxin Channel.

The remarkable switching of conformation in the presence of detergents or phospholipid vesicles suggests that pardaxin is a very flexible molecule. This property helps to explain the apparent ability of pardaxin to insert into phospholipid bilayers.

The channel model we favor is comprised of 12 antiparallel monomers (Fig. 6); however, similar structures comprised of eight or ten monomers cannot be excluded. The kinetics of pore formation in liposomes and the dependence of planar bilayer conductance on toxin concentration yield linear relationships with slopes around 8-12. The

common interpreation of such results is that an aggregate of 8-12 molecules forms the ion conducting channel. Antiparallel models appear to be more probable because they allow: 1) The interaction of negative carboxyls of the C-terminus glutamate with positive charges of Lys-16 and Lys-8; 2) the favorable interaction of the backbone dipoles of adjacent C-helices; 3) the only negatively charged portion of the molecule, the C-terminus, to lie near to the radial center of the pore where it could make the channel selective to cations; and 4) large hydrophobic side chains on the C-helix to pack tightly next to each other. Models in which the monomers are parallel, appear unlikely because: 1) all models with parallel helices have highly positively charged regions that should strongly reduce cation permeability; and 2) we could find no parallel models in which side chains pack next to each other as well as they pack in antiparallel models. C-helices pack very closely in an antiparallel manner to form a dimer with the following features: all the large alkyl side chains and the phenlyalanine side chain from a two-residue-wide hydrophobic column on one side of the dimer, while on the opposide side of the dimer the several serines form hydrogen bonds with each other. In addition, the points of closest contact between helix backbones are Gly-23 and Gly-30, the positively charged Lys-16 extends over the C-terminus of the adjacent helix where it interacts favorably with the negative end of the helix dipole and carboxyls of the terminus Glu-33, and the helices cross each other at an angle of -15 degrees predicted by '3-4 ridges into grooves' helix packing theory. This dimer for the C-helices was used to construct models of pardaxin in solution as a tetramer (Fig. 2) on the membrane surface as a "raftlike" structure

(data not shown), and in the transmembrane orientation as a channel (Fig. 6a).

In constructing the channel (as a 12-mer) (Fig. 6a), C-helices of the initial dimers were packed next to each other so that Ala-21 and Ala-25 packed between each other and a hydrogen bonded forms between Thr-17 and Ser-29. The helices crossed at an angle of 25 degrees. This packing is similiar to that of "4-4 ridges-into-grooves" packing; however, the "ridge" formed by side chains four residues apart packed on top of each other instead of between each other. This is possible because the alanine side chains are small.

This model has narrow regions near its entrances that should control the ion selectively and a large non-charged pore through the rest of the membrane. Figure 6B shows the entrance of the channel formed by residues 1-16 and 31-33. These segments contain all the charged groups. The N-helices form a hydrophobic and positively charged outer ring that surrounds the negatively charged C-termini. The narrowest portion of the channel is formed by a ring of six amide groups from the Gln-32 side chains. These form a network of hydrogen bonds with each other and with the carboxy termini. Lys-8 and Lys-16 form salt bridges to the two carboxyl groups of Glu-33. The cation selectivity of the channel is probably due to the fact that: the amine groups are farther from the center of the channel than are the carboxyl groups, the C-terminus of the C-helix is nearer the channel entrance than is its N-terminus, the narrow opening is lined by oxygens from the Gln-32 amide groups, and the positive charges of the

N-termini may interact with negatively charged lipid head groups. A sphere of diameter 4.8 angstrom could just pass through this ring. This is large enough to pass the known permeant cations but small enough to exclude Tris, which is impermeant. The ring is just the size to bind a lithium cation hydrated by six water molecules each of which can form up to two hydrogen bonds with the oxygens of the Gln amide groups.

The central region of the channel formed by residues 17-30 is shown in Figure 6C. Only serine side chains line the hexagonally-shaped pore. The pore is about 20 angstroms wide. The exterior of the structure which would be exposed to lipid contains only alkyl side chains. The channel is large enough to contain an hexagonally shaped Ice I type water structure in which each cross-sectional "layer" of water molecules contains 42 water molecules. The hydroxyl groups of the channel lining may interact with this or a similar kind of water structure that has 3- or 6-fold symmetry.

The most likely way for pardaxin molecules to insert across the membrane in an antiparallel manner is for them to form antiparallel aggregates on the membrane surface that then insert across the membrane. We developed a "raft" model (data not shown) that is similar to the channel model except that adjacent dimers are related to each other by a linear translation instead of a 60 degree rotation about a channel axis. All of the large hydrophobic side chains of the C-helices are on one side of the "raft" and all hydrophilic side

chains are on the other side. We postulate that these "rafts" displace the lipid molecules on one side of the bilayer. When two or more "rafts" meet they can insert across the membrane to form a channel in a way that never exposes the hydrophilic side chains to the lipid alkyl chains. The conformational change from the "raft" to the channel structure primarily involves a pivoting motion about the "ridge" of side chains formed by Thr-17, Ala-21, Ala-25 and Ser-29. These small side chains present few steric barriers for the postulated conformational change.

6. Conclusions.

Pardaxin is the principal polypeptide toxic component of the secretion of the flatfish Pardachirus marmoratus. It is secreted into the water by a series of double, clindrical acinar glands. Although it is water soluble, at concentrations of 10^{-7} - 10^{-11} M, this polypeptide spontaneously inserts into artificial or biological membranes to form voltage gated pores which are permeable to cations and anions. At concentrations higher than 10^{-7} M pardaxin acts as a lytic agent. Both properties probably underly the toxicity and repellency to marine organisms. The primary sequence of pardaxin, elucidated for the first time in the present study, indicates a strong hydrophobic segment at the amino-terminal, followed by an α-helical amphipathic region and a hydrophylic carboxy terminal.

In analogy to a series of polypeptide channel forming quasi ionophores, a model of pardaxin tetramer in water and in the membrane

is presented: 1) In aqueous buffer pardaxin is tightly packed and is comprised of four antiparallel monomers with 2-fold symmetry of the "4-4 ridges into grooves" type; the hydrophobic amino-terminal segments of pardaxin monomers are shielded from the aqueous surface in the tetramer which most probably exposes the polar side chain to water; 2) interaction with a lipid bilayer driven by polar and/or hydrophobic forces between the amino acid side chains of the pardaxin tetramers and the polar membrane lipid head group triggers insertion from a "raft" like structure; 3) in the bilayer or upon interaction with detergent micelles, a structural reorganization of pardaxin aggregates takes place, in which the polar side chains interact with themselves and the hydrophobic residues are externally oriented in pardaxin aggregate, therefore allowing interactions with the lipid backbone hydrocarbons; 4) in this pardaxin oligomer channel the helices cross at an angle of 25 degrees and the model predicts an cation selective hydrophilic interior allowing for passage of ions; 5) the voltage induces the opening of pardaxin pores, or opens them indirectly, by affecting pardaxin oligomers, supposed to be stabilized by dipoledipole interactions of monomer helices; 6) most probably the presence of pardaxin pores alters the structure of the bilayer resulting with phosphatidylserine vesicles aggregation, mediated by contact but not by partial merging of their membranes.

List of publications arising from ONR-supported Research on pardaxin (1985-1988)

1. Lazarovici, P., Primor, N., Gennaro, J., Fox, J., Shai, Y., Lelkes, P.I., Canatsch, C.G., Raghunathan, G., Guy, H.R., Shih, Y.C. and Edwards, C. Origin, chemistry and mechanisms of action of pardaxin, a repellent, presynaptic exitatory, ionophore polypeptide. In Marine Toxins (S. Hall, ed.) American Chemical Society, Washington, D.C. In press.

2. Lelkes P. and Lazarovici P. Pardaxin induces aggregation but no fusion of phosphatidyeserine vesicles. Febs Lett. 230, 131-136, 1988.

3. Renner, P., C.G. Caratsch, P.G. Waser, P. Lazarovici and N. Primor. Presynaptic effects of the pardaxins, polypeptides isolated from the gland secretion of the flatfish Pardachirus marmoratus. Neuroscience 23, 319-325, 1987.

4. Van Praag, D., S. J. Farber, E. Minkin and N. Primor. The production of eicosanoids by the killifish gills and operculum epithelia and their effect on active transport of ions. Gen. Endocrinol. 67, 50-57, 1987.

5. Lazarovici, P., N. Primor and L. M. Loew. Purification and pore forming activity of two hydrophobic polypeptides from the secretion of the Red Sea Moses sole (Pardachirus marmoratus). J. Biol. Chem. 261, 16704-16713,1986.

6. Primor, N. Action on ileal smooth muscle of synthetic detergents and pardaxin. Gen. Pharmocol. 17: 413-418, 1986.

7. Primor, N. Pharyngeal cavity and the gills are the target oran for the repellent action of pardaxin in shark. Experientia. 41: 693-696, 1985.

8. Moran, A., Z. Korchack, N. Moran and N. Primor. Formation of Transmembrane channels in lipid bilayers by the surfactant-like toxin from the Red Sea flatfish Pardachirus marmoratus. In: Toxins, drugs and pollutants in marine animals. (Eds. L. Bolis, J. Zadunaisky and R. Gilles). Springer-Verlag, Berlin, 1985

FIGURE LEGENDS

Figure 1: Pardachirus marmoratus fish and the morphology of the toxin secretory glands.

a,b - Lateral views of the fish. Arrows indicate white secretion around the gland openings.

c - Photomicrograph (20X) of the two toxin secreting glands in sagittal section. The glands (g), are right of the ray articulation (a) and are filled with secretion. The clear space within each gland lies in the secretory duct(s) (d) which end out of the image to the right.

d - An electronmicrograph (30,000X) of the glandular secretory epithelium and a portion of one acinus. Peripheral to the area of moderately electron dense material (SC) which is the toxic secretion(s), is the thin secretory epithelial cell (fsc). Several secretory vesicles (bse) can be seen on its surface, some separated from the contents of the acinar pool only by the thickness of the plasma membrane.

e - An electronmicrograph (80,000X) showing the secretory cell cytoplasm in detail. The fibrillar nature of the cytoplasmic matrix is visible as well as the smooth (agranular) appearance of the endoplasmic membranes. Mitochondria (m) can be seen and a portion of one of the plasma membrane elevations within which is a material of almost identical granularity and electron density to that in the acinar pool. No secretory granules are visible in the cytoplasm.

f - This electronmicrograph (20,000X) is an image of the cells lining the secretory duct (d). Their rounded apical elevations (ae) project into the secretory space and come into contact with the secretion.

Figure 2: **Computer graphic stereo views of pardaxin tetramer in aqueous solvents.**

a - The front center portions of the green and yellow monomers are the long amphipathic α helices that cross at an angle of 15° predicted by "3-4 ridges-into-grooves" helix packing, as in the channel model. Helices of the green and yellow dimer cross those of the blue and purple dimer by an angle of 40°, consistent with "4-4 ridges-into-grooves" helix packing. This places the two-residue-wide hydrophobic strip on each dimer next to each other. The N-helices of each monomer fit into hydrophobic grooves and interact with the hydrophobic strips on each side of the tetramer.

b - The tetramer viewed from the top. The transition segment between the N-helix and the C-helix is shown in yellow and blue and the C-terminus is shown in green and purple. The hydrophobic strips are in the center and the N-helices are on each side. The tetramer has 2-fold symmetry about each of the three axes.

Figure 3: **The effect of pardaxin on the short circuit current of the isolated epithelial preparations.**

a - Isolated skin of the frog R. catesbeiana. Pardaxin (6×10^{-5} M) was applied to the mucosal side. ADH (5×10^{-7} M) was applied to the serosal side.

b - Isolated opercular skin of seawater-adapted killifish E. heteroclitus. Pardaxin (10^{-5} M) (full line) and melittin (3×10^{-5}/circles) were added (first arrow) to the mucosal (seawater) side of the skin. Isoprenaline (2×10^{-6} M) was added to the serosal side (second arrow). The tracing is a continuous short-circuit current

(Isc).

Figure 4: **Effect of pardaxin on intracellular ionized calcium level in bovine adrenal chromaffin cells.**

Isolated chromaffin cells were maintained in suspension culture and loaded with the fluorescent calcium indicator Fura 2 as previously described (28). 2 x 10^5 cells/ml were added into a cuvette containing standard buffer without (dotted line) or with (full line) 2 mM calcium. At the arrow, 10^{-7} M pardaxin was added. Only in the presence of calcium a rise in $[Ca^{2+}]_{in}$ was observed. Inset - typical control experiment. Depolarization of the cells by 30 mM KCl resulted in rapid increase in $[Ca^{2+}]_{in}$. Further, addition of 0.1 μM ionomycin, a calcium ionophore, increased to saturation the intracellular calcium level.

Figure 5: **Scheme of the bilayer formation at the tip of the patch pipets (A) and single channel recordings of pardaxin pores (B).**

A - Step 1 - Monolayer of phosphatidylethanolamine is prepared at the air water interface with a glass road; Step 2 - A patch pipet is removed from the solution, the lipid headgroups of the monolayer are attached while the fatty acids hydrophobic tail is exposed to the air; Step 3 - The pipet is reinserted into the liquid, resulting in apposition of the hydrocarbon tails of the attached monolayer to those of the original monolayer, forming a bilayer (27); Step 4- Addition of the synthetic pardaxin (10^{-9} M) to the bath results in about 30 min with spontaneous tetramers insertion into the bilayer and pore formation as measured by the current fluctuations represented in B at a positive potential of 100 mV. The single

channel conductance can be estimated from the amplitude of the current steps divided by the applied voltage and was in the range of 16 pS.

Figure 6: **Computer graphic stereo views of pardaxin channel model.**

A - Side view of one-half (six monomers) of the channel as seen from inside the channel. Monomers with the N-termini on top are white, those with the N-termini on the bottom are green. Polar side chain atoms are colored red for negatively charged carboxyls, blue for positively charged amines, pink for hydroxyls and oxygen of amides, and cyan for nitrogen of amides. N-helices are horizontal and form an outer ring around the entrance of the channel; C-helices are vertical and form the walls of the pore. Side chains of Glu-32 near the C-terminus extend toward the center of the pore to form narrow ion selective regions near each entrance.

B - Top view of channel entrance formed by residues 1-16 (white outer segments) and residues 31-33 (green inner segments). Note central ring formed by amide groups of Gln-32 side chains (pink and light blue) and salt bridges between carboxy groups of Glu-33 (red) and amine groups (dark blue).

C - Central region of the channel formed by residues 17-30. C-helices with N-termini pointing out of the page are white, those with N-termini pointing in are green. Hydroxyl groups are pink. The hexagonal opening is about 11 angstroms on each side.

Fig. 1

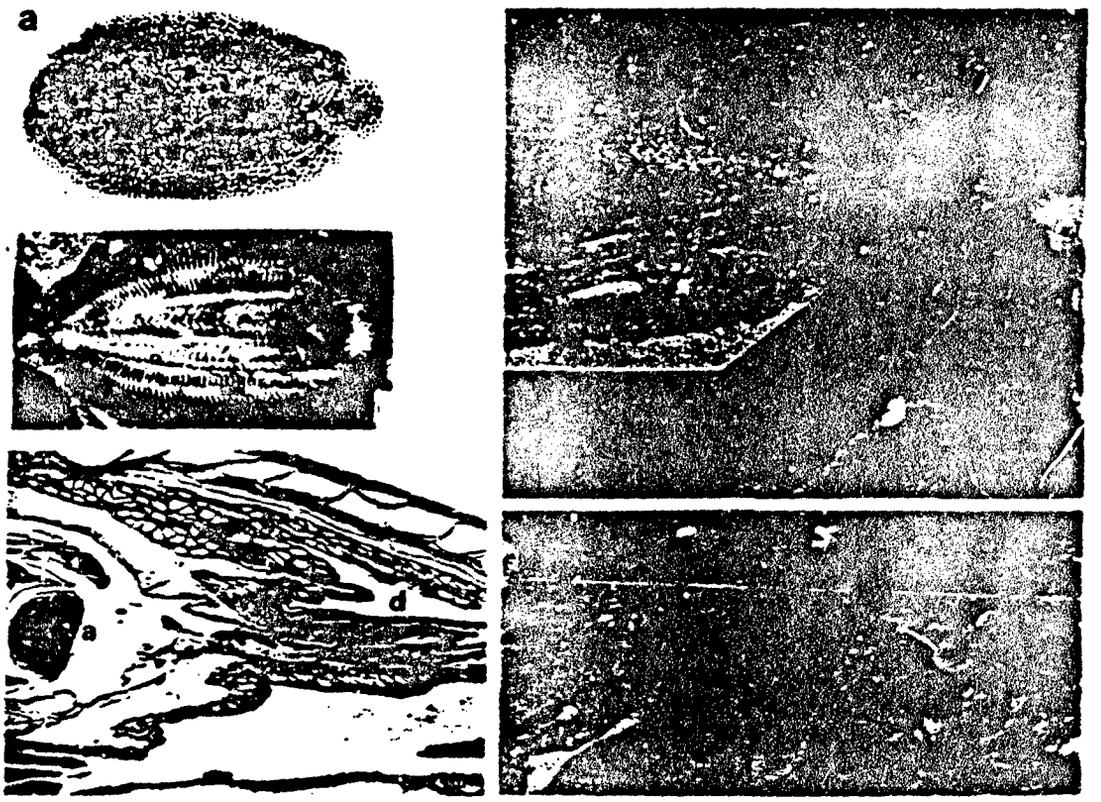

Fig. 2

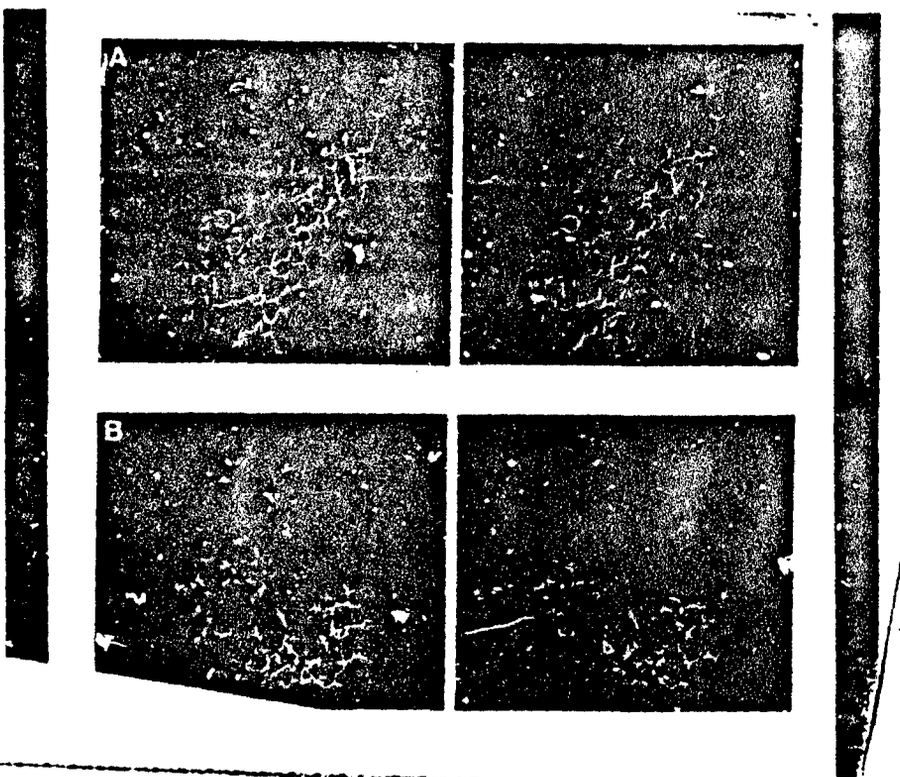

Fig. 3

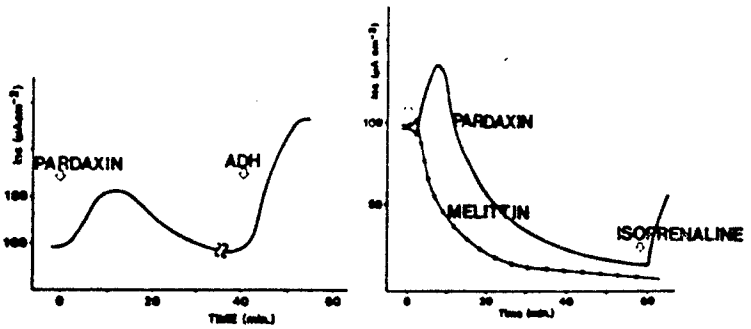
PARDAXIN
ADH
PARDAXIN
MELITTIN
ISOPRENALINE

Fig. 4

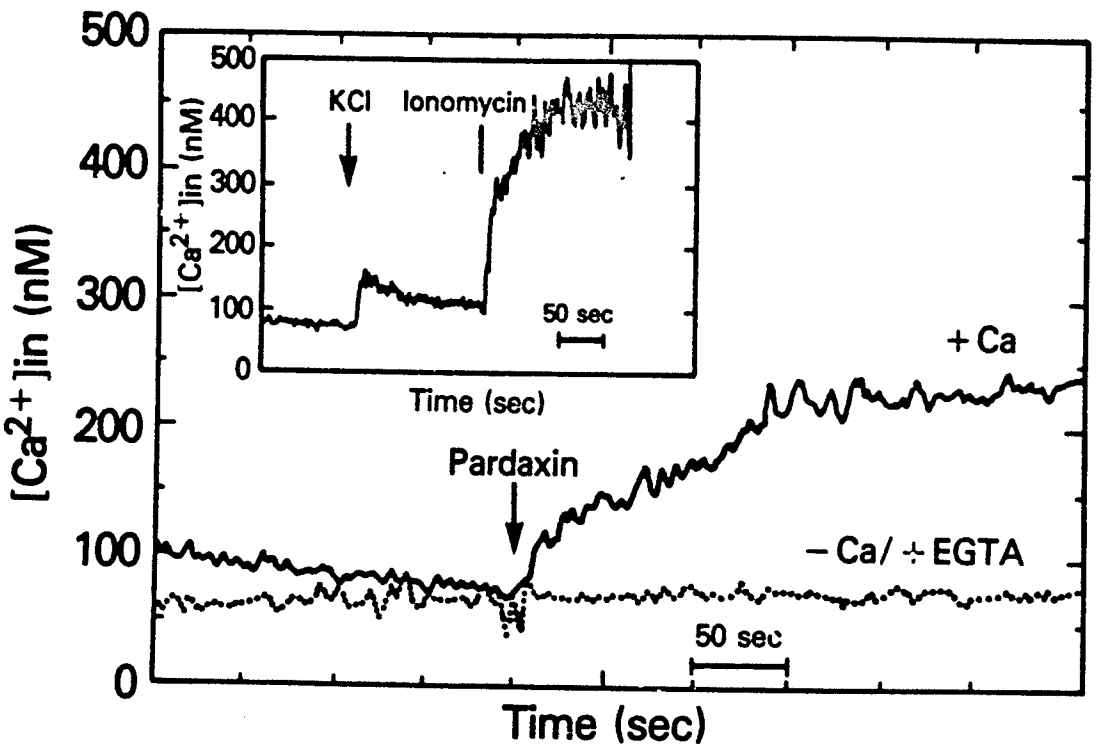
500
400
300
200
100
0
[Ca2+]in (nM)
KCl
Ionomycin
50 sec
Time (sec)
+Ca
Pardaxin
−Ca/÷EGTA
50 sec
Time (sec)

Fig. 5

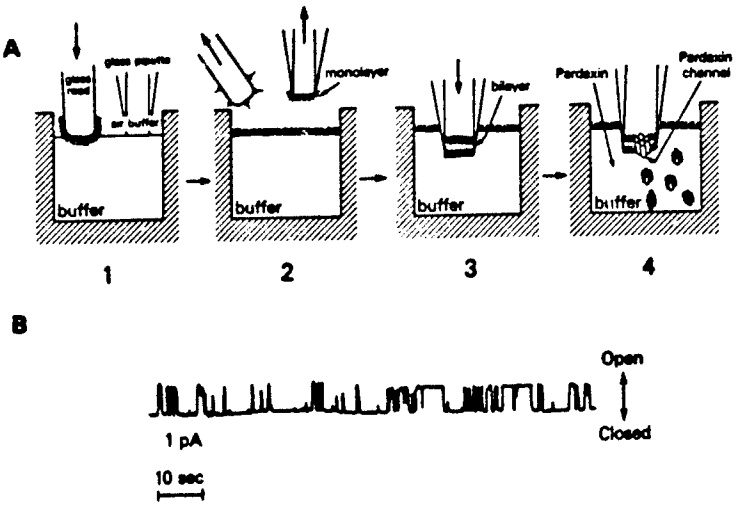
A
buffer
monolayer
bilayer
Perdaxin
Perdaxin channel
1
2
3
4
B
Open
Closed
1 pA
10 sec

Fig. 6

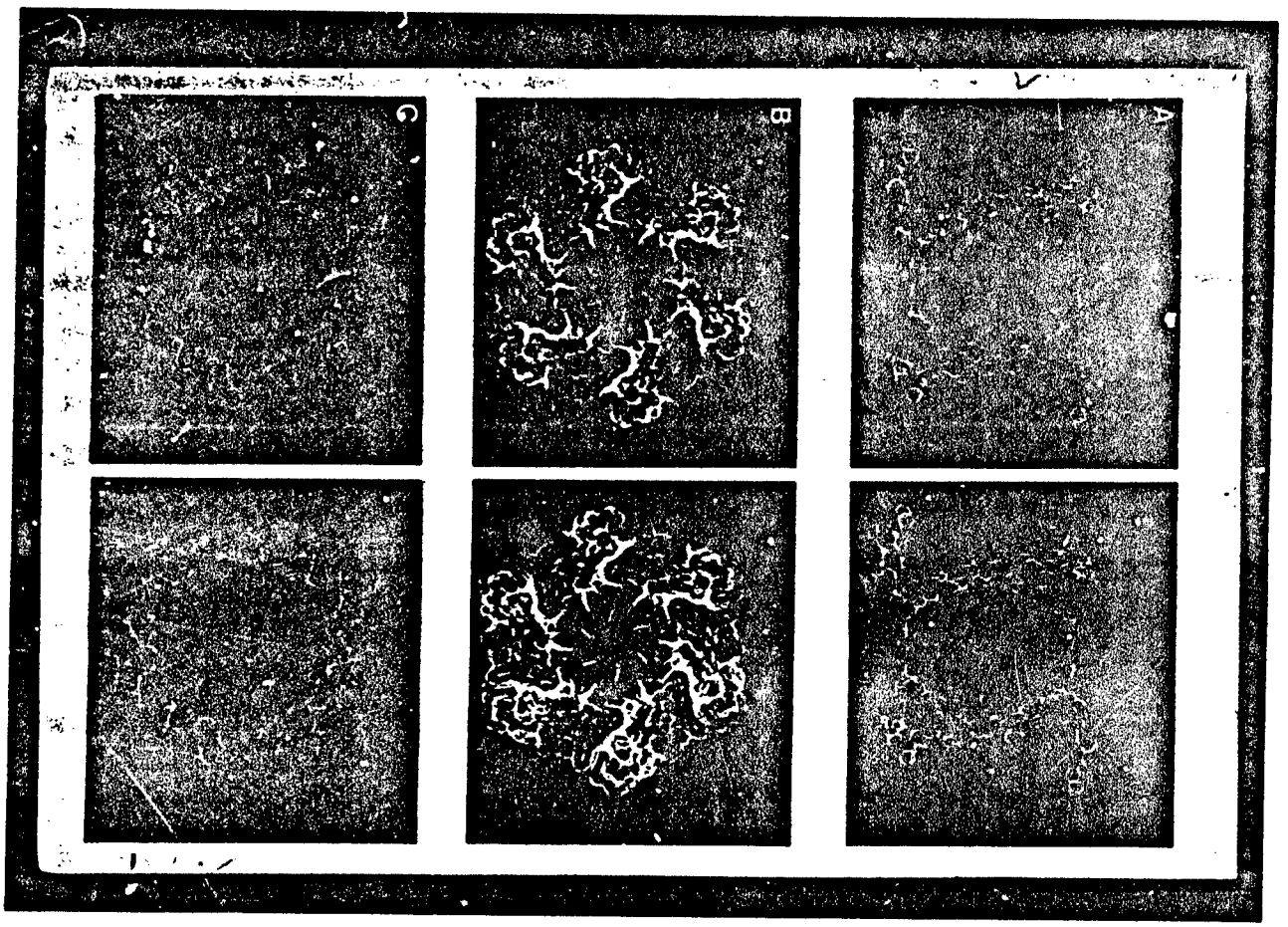
C
B
A